

**Effects of pressure on enzyme function of *Escherichia coli*  
dihydrofolate reductase**

**Eiji Ohmae <sup>a</sup>, Mineyuki Tatsuta <sup>a</sup>, Fumiyoshi Abe <sup>b</sup>, Chiaki Kato <sup>b</sup>,  
Naoki Tanaka <sup>c</sup>, Shigeru Kunugi <sup>c</sup>, Kunihiko Gekko <sup>a,\*</sup>**

<sup>a</sup> *Department of Mathematical and Life Sciences, Graduate School of Science,  
Hiroshima University, Higashi-Hiroshima 739-8526, Japan*

<sup>b</sup> *Extremobiosphere Research Center, Japan Marine Science and Technology  
Center (JAMSTEC), Yokosuka 237-0061, Japan*

<sup>c</sup> *Department of Polymer Science and Engineering, Kyoto Institute of  
Technology, Kyoto 606-8585, Japan*

Running title: Effects of pressure on DHFR function

---

Abbreviations: DHFR, dihydrofolate reductase; DHF, dihydrofolate; NADPH, nicotinamide adenine dinucleotide phosphate (reduced form); NADPD, [4'(*R*)-<sup>2</sup>H]NADPH; THF, tetrahydrofolate.

\* Corresponding author. Fax: +81-82-424-7327;  
E-mail: gekko@sci.hiroshima-u.ac.jp

## Abstract

To elucidate the effects of pressure on the function of *Escherichia coli* dihydrofolate reductase (DHFR), the enzyme activity and the dissociation constants of substrates and cofactors were measured at pressures up to 250 MPa at 25°C and pH 7.0. The enzyme activity decreased with increasing pressure, accompanying the activation volume of 7.8 ml mol<sup>-1</sup>. The values of the Michaelis constant ( $K_m$ ) for dihydrofolate and NADPH were slightly higher at 200 MPa than at atmospheric pressure. The hydride-transfer step was insensitive to pressure, as monitored by the effects of the deuterium isotope of NADPH on the reaction velocity. The dissociation constants of substrates and cofactors increased with pressure, producing volume reductions from 6.5 ml mol<sup>-1</sup> (tetrahydrofolate) to 33.5 ml mol<sup>-1</sup> (NADPH). However, the changes in Gibbs free energy with dissociation of many ligands showed different pressure dependences below and above 50 MPa, suggesting conformational changes of the enzyme at high pressure. The enzyme function at high pressure is discussed based on the volume levels of the intermediates and the candidates for the rate-limiting process.

*Keywords:* Dihydrofolate reductase; Enzyme activity; High pressure; Volume change

## 1. Introduction

Dihydrofolate reductase (DHFR, EC 1.5.1.3) catalyzes the reduction of dihydrofolate (DHF) to tetrahydrofolate (THF) by using the cofactor nicotinamide adenine dinucleotide phosphate (NADPH). The product, THF, is a precursor of a cofactor that is important in the biosynthesis of purine nucleotides and some amino acids, making DHFR an essential enzyme for all living organisms. As shown in Fig. 1, DHFR from *Escherichia coli* consists of four  $\alpha$ -helices, eight  $\beta$ -strands, and four flexible loops (Met20,  $\beta$ C- $\beta$ D,  $\beta$ F- $\beta$ G, and  $\beta$ G- $\beta$ H) [1, 2]. These loops actively and cooperatively fluctuate in order to accommodate the substrate and cofactor. In crystals, the catalytic Met20 loop has ‘open’, ‘closed’, and ‘occluded’ conformations, depending on whether it binds the substrate (or a substrate analogue), the cofactor, or both [2]. A high-pressure NMR study revealed that increasing the pressure transforms the conformation of a catalytic Met20 loop from the ‘closed’ to the ‘open’ form in a DHFR•folate complex [3]. Site-directed mutation studies have demonstrated that the other three loops also play important roles in the stability and function of this enzyme [4–6]. These studies indicate that the enzymatic function of DHFR is directly linked to its structural dynamics. The relationship between the structural dynamics and function of DHFR has been reviewed by Schnell *et al.* [1].

(Fig. 1)

A high-pressure experiment is a novel method of evaluating the volume changes of a reaction pathway, yielding useful information on the mechanisms of an enzyme reaction. Therefore, the reaction kinetics of many enzymes have been examined by various spectroscopic techniques under conditions of hydrostatic pressure [7–11]. However, this methodology has not been applied to DHFR because its enzyme kinetics involves many ligand-binding and -releasing processes, and because the conformational change of the enzyme may occur at high pressure. Fierke *et al.* [12] indicated that the reaction kinetics of DHFR involves five main intermediates, as shown in Scheme 1:  $\text{DHFR} \cdot \text{NADPH} \rightarrow \text{DHFR} \cdot \text{NADPH} \cdot \text{DHF} \rightarrow \text{DHFR} \cdot \text{NADP}^+ \cdot \text{THF} \rightarrow \text{DHFR} \cdot \text{THF} \rightarrow \text{DHFR} \cdot \text{NADPH} \cdot \text{THF}$ ; and involves many equilibrium

states such as DHFR•NADP<sup>+</sup>. In this cycle, the ternary complex DHFR•NADPH•DHF is a transient state due to the very rapid hydride transfer from NADPH to DHF. The adiabatic compressibility (volume fluctuation) of these intermediates changes with the reaction coordinate and the comparable changes in internal cavities, with the transient state being the most flexible and DHFR•NADP<sup>+</sup>•THF being the most rigid [13]. Recently, Boehr *et al.* used an NMR relaxation dispersion method to reveal that the maximum hydride-transfer and steady-state turnover rates of this enzyme are governed by the dynamics of transitions between the ground and excited states [14].

(Scheme 1)

In a recent preliminary study [15], we found that the activity of *E. coli* DHFR decreases with increasing pressure, whereas *Shewanella violacea* DHFR isolated from the Ryukyu Trench at a depth of 5,110 m has an optimal activity at around 100 MPa. This represents evidence that the characteristic pressure susceptibility and structural dynamics of DHFRs differ between deep-sea bacteria and living organisms at atmospheric pressure. Therefore, a systematic investigation of the effects of pressure on DHFRs should give new insight into the protein dynamics and pressure-adaptation mechanisms of deep-sea proteins. To initiate such an investigation, in the present study we examined the effects of pressure on the enzyme activity and dissociation constants of substrate and cofactor of *E. coli* DHFR at pressures up to 250 MPa. The enzyme function at high pressure is discussed based on the volume levels of the intermediates and the candidates for the rate-limiting process.

## 2. Materials and Methods

### 2.1. Protein purification

DHFR was purified from *E. coli* strain HB101 containing overexpression plasmid pTZwt1-3 [16], according to previously described procedures [5, 6]. For high-pressure experiments, the purified DHFR solution (10 mM

phosphate) was exhaustively dialyzed against 20 mM Tris-hydrochloride buffer (pH 7.0). The concentration of DHFR was determined by absorption measurements on a spectrophotometer (Jasco V-560), using a molar extinction coefficient of 31,100 M<sup>-1</sup> cm<sup>-1</sup> at 280 nm [12].

## *2.2. Steady-state kinetics at atmospheric pressure*

The steady-state kinetics of the enzyme reaction at atmospheric pressure were studied spectrophotometrically at 25.0°C as described previously [4–6]. The buffer used was 20 mM Tris-hydrochloride (pH 7.0) containing 0.1 mM EDTA and 0.1 mM dithiothreitol. The concentrations of DHF (Sigma) and NADPH (Oriental Yeast) were determined spectrophotometrically using molar extinction coefficients of 28,000 M<sup>-1</sup> cm<sup>-1</sup> at 282 nm and 6,200 M<sup>-1</sup> cm<sup>-1</sup> at 339 nm, respectively [17]. The Michaelis constant ( $K_m$ ) and the rate constant of catalysis ( $k_{cat}$ ) for DHF were measured for various concentrations of DHF (0.3–50 μM) at a saturated concentration of NADPH (50 μM). The  $K_m$  and  $k_{cat}$  values for NADPH were measured for various concentrations of NADPH (0.3–50 μM) at a saturated concentration of DHF (50 μM). In both experiments, the enzyme concentration was determined by the methotrexate titration method [18] to eliminate the effects of denatured species that may be produced during storage. The initial velocities ( $v$ ) of the enzyme reaction were calculated from the time course of absorbance at 340 nm using a differential molar extinction coefficient of 11,800 M<sup>-1</sup> cm<sup>-1</sup> [19]. The obtained data were fitted to the following equation by nonlinear least-squares analysis with the Origin program:

$$v = (k_{cat} [E] [S]) / (K_m + [S]) \quad (1)$$

where [E] is the enzyme concentration and [S] is the initial substrate concentration.

## *2.3. Pressure dependence of enzyme activity*

The pressure dependence of the enzyme activity was measured using a spectrophotometer (Shimadzu UV-1600PC) equipped with a high-pressure

absorbance cell unit (Teramecs PCI-400) and a hand pump (Teramecs PCI-500). The temperature was controlled to 25.0°C with a circulating thermobath (NESLAB RTE-111). The buffer used was 20 mM Tris-hydrochloride (pH 7.0) containing 0.1 mM EDTA and 0.1 mM dithiothreitol. The enzyme reaction was started by mixing the DHF solution with the enzyme•NADPH solution in a 2-ml microtube at final concentrations of enzyme (10 nM), NADPH (250 μM), and DHF (250 μM). Before mixing, both solutions were preincubated for 10 min to equilibrate the temperature and eliminate the hysteresis effect [20]. The reaction mixture was loaded into the high-pressure cell, and the absorbance was measured for 1–5 min after pressurization to the desired pressure. The initial velocities of the enzyme reaction were calculated from the time course of the absorbance at 370 nm using the differential molar extinction coefficient at each pressure (e.g., 3,180 and 3,710 M<sup>-1</sup> cm<sup>-1</sup> at 0.1 and 250 MPa, respectively), which was predetermined from the differences in the absorbance spectra for the substrates (NADPH and DHF) and the products (NADP<sup>+</sup> and THF). The activation free energy ( $\Delta G^*$ ) and the activation volume ( $\Delta V^*$ ) of the enzyme reaction were calculated using the following equation, which is applicable at the saturated substrate concentration:

$$\begin{aligned}
 \Delta V^* &= (\partial \Delta G^* / \partial P)_T = [\partial (-RT \ln k_{cat}) / \partial P]_T \\
 &= [\partial (-RT \ln v_{max}) / \partial P]_T - [\partial (-RT \ln [E]) / \partial P]_T \\
 &= [\partial (-RT \ln v) / \partial P]_T
 \end{aligned} \tag{2}$$

where  $R$  is the gas constant,  $T$  is the absolute temperature,  $P$  is the pressure, and  $v_{max}$  is the maximum velocity.

The apparent  $K_m$  values for DHF and NADPH were estimated from the progressive curve of absorbance at 340 nm at 0.1 and 200 MPa using the enzyme concentrations of 3 and 5 nM, respectively [21, 22]. To minimize reverse reactions and product inhibition, the initial concentrations of DHF and NADPH were 30 and 80 μM. The observed absorbance at time  $t$ ,  $A_t$ , was directly fitted to the following equations using the SALS program [23]:

$$A_t = A + \Delta \epsilon [S]_t \tag{3}$$

$$[S]_t = [S]_{t-\Delta t} - v_{\max} [S]_{t-\Delta t} \Delta t / (K_m + [S]_{t-\Delta t}) \quad (4)$$

where  $[S]_t$  is the concentration of free substrate at time  $t$ ,  $\Delta t$  is the time interval of measurements (0.5 s in this experiment),  $v_{\max}$  is the maximum velocity, and  $\Delta \epsilon$  is the differential molar extinction coefficient (11,800 and 12,050  $\text{M}^{-1} \text{cm}^{-1}$  at 0.1 and 200 MPa, respectively).

#### 2.4. Effects of deuterium isotope

[4'(R)- $^2\text{H}$ ]NADPH (NADPD) was prepared by the method described previously [5]. The enzyme activities were measured at various pressures using NADPD (250  $\mu\text{M}$ ) instead of NADPH as described above. The effect of the deuterium isotope,  $^D v$ , was calculated with the following equation since  $k_{\text{cat}}$  is proportional to  $v$  under the experimental conditions used:

$$^D v = v^{\text{NADPH}} / v^{\text{NADPD}} \quad (5)$$

where  $v^{\text{NADPH}}$  and  $v^{\text{NADPD}}$  are the initial velocities of the enzyme reaction measured using NADPH and NADPD as the coenzyme, respectively.

#### 2.5. Dissociation constants of ligands

The values of the equilibrium dissociation constant ( $K_d$ ) of ligands (substrate and coenzyme) from the enzyme were determined from the ligand concentration dependence of tryptophan fluorescence of the enzyme at various pressures, using a spectrofluorometer (Shimadzu RF-5000) equipped with a high-pressure fluorescence cell unit (Teramecs PCI-400SRF) and a hand pump (Teramecs PCI-500). The temperature was controlled to 25.0°C with a circulating thermobath (NESLAB RTE-111). The solvent used was 20 mM Tris-hydrochloride (pH 7.0) containing 0.1 mM EDTA and 0.1 mM dithiothreitol. The emission spectra for excitation at 290 nm were measured at 280–500 nm for an enzyme concentration of about 7  $\mu\text{M}$ . The fluorescence intensities ( $F$ ) at the peak wavelengths of the 0.1-MPa spectra were plotted against the ligand concentrations and fitted to the following equation with the Origin program:

$$F = F_0 [E] + \Delta F \left\{ [E] + [L] + K_d - \sqrt{([E] + [L] + K_d)^2 - 4[E][L]} \right\} / 2 \quad (6)$$

where  $F_0$  is the molar fluorescence intensity of the enzyme without ligand,  $\Delta F$  is the difference in molar fluorescence intensities between the free enzyme and the enzyme•ligand complex, and  $[E]$  and  $[L]$  are the concentrations of enzyme and ligand, respectively. The  $K_d$  values for the dissociation of substrate (folate and THF) from the DHFR•NADPH•substrate ternary complexes were calculated from the fluorescence peak (443 or 444 nm) induced by the addition of 100  $\mu$ M NADPH. The  $K_d$  value for the dissociation of NADPH from the DHFR•NADPH•substrate ternary complexes was calculated by linked function analysis according to the thermodynamics of cyclic equilibria with the individual  $K_d$  values along the conceivable reaction paths, the dissociation of substrate and NADPH from the binary complexes, and the dissociation of substrate from the ternary complex. The Gibbs free energy change ( $\Delta G_d$ ) and the partial molar volume change of dissociation ( $\Delta V_d$ ) were calculated as follows:

$$\Delta V_d = (\partial \Delta G_d / \partial P)_{T=} [\partial (-RT \ln K_d) / \partial P]_{T=} \quad (7)$$

### 3. Results

#### 3.1. Pressure dependence of enzyme activity

Figure 2 shows the time courses of absorbance at 370 nm associated with the enzyme reaction of DHFR at various pressures. The reaction process could be continuously monitored for at least 5 min after starting data collection due to the use of high concentrations (250  $\mu$ M) of substrate and coenzyme, which allowed us to estimate the initial velocity of the enzyme reaction. The slope of the absorbance change obviously decreased with increasing pressure, indicating reduced enzyme function at higher pressure. This was neither due to irreversible or reversible pressure denaturation of



DHFR, since the time course of the absorbance showed similar slopes at 0.1 MPa before and after pressurization to 250 MPa (Fig. 2), and since no evidence of a denatured form was observed by high-pressure NMR analysis [3] at the pressures examined (<200 MPa).

(Fig. 2)

As shown in the inset of Fig. 2, the  $\Delta G^*$  values decreased linearly with increasing pressure. The activation volume,  $\Delta V^*$ , was estimated from the slope as  $7.8 \pm 0.6$  ml mol<sup>-1</sup> (mean  $\pm$  SD). This value is close to our previous estimate of  $8.1 \pm 0.8$  ml mol<sup>-1</sup>, although the concentrations of substrate and coenzyme differed [15]. The positive  $\Delta V^*$  value indicates that a rate-limiting step in the reaction pathway of DHFR accompanies a volume increase of the protein.

The pressure depression mechanism of enzyme function could be understood in more detail through the effects of pressure on the kinetics parameters,  $K_m$  and  $k_{cat}$ . However, directly determining these parameters at high pressure was difficult under our experimental conditions because a stopped-flow apparatus was necessary for measuring the wide range of the initial velocities of the enzyme reaction at high pressure. Therefore, the apparent  $K_m$  and  $v_{max}$  values were conventionally estimated from the entire time courses of the absorbances at 0.1 and 200 MPa. As shown in Fig. 3, the absorbance at 340 nm decreased with time at the two concentrations of NADPH and DHF. These time courses were satisfactorily fitted to Eqs. 3 and 4 with the parameter values listed in Table 1. The obtained  $K_m$  values at 0.1 MPa were considerably larger than our previous data in succinate-imidazole-diethanolamine buffer:  $1.1 \pm 0.3$   $\mu$ M for NADPH and  $1.3 \pm 0.1$   $\mu$ M for DHF [5]. Similar  $K_m$  values ( $1.6 \pm 0.2$   $\mu$ M for NADPH and  $0.9 \pm 0.1$   $\mu$ M for DHF) were also obtained from the steady-state kinetics experiments at 0.1 MPa in Tris-hydrochloride buffer as used in high-pressure experiments. The use of the conventional method would overestimate the  $K_m$  values probably due to the presence of some reverse reaction and/or product inhibition in accordance with the enzyme reaction. However, since the obtained  $K_m$  values were much smaller than the concentrations of NADPH and DHF (250  $\mu$ M) used in the activity

measurements (Fig. 2), we can conclude that the  $K_m$  values for NADPH and DHF are slightly larger at 200 MPa than at 0.1 MPa, and hence that the affinity of these ligands for enzyme is somewhat depressed at high pressure. On the other hand, the  $v_{\max}$  values obtained for NADPH (164 nM s<sup>-1</sup>) and DHF (95 nM s<sup>-1</sup>) were almost the same at 0.1 and 200 MPa (Table 1), even though the enzyme concentration used in the 200-MPa experiments was about twice of that in the 0.1-MPa experiments. This result suggests that the  $k_{\text{cat}}$  value of DHFR decreases with pressure, and hence that the pressure-induced depression of enzyme function is due to unfavorable effects of pressure on both  $K_m$  and  $k_{\text{cat}}$ , with the latter being dominantly affected.

(Fig. 3) (Table 1)

### 3.2. Effect of deuterium isotope on hydride transfer

To examine the effects of pressure on the hydride-transfer process, the enzyme reaction was measured using NADPD instead of NADPH at various pressures below 250 MPa. The obtained  $^Dv$  values are listed in Table 2. When the hydride transfer is the rate-limiting step, the rate of hydride transfer for NADPD should be one-third of that for NADPH ( $^Dv = 3$ ) [12]. However, the obtained  $^Dv$  values were 1.1–1.2 at all pressures examined, indicating that the hydride transfer is not a rate-limiting step and is not substantially affected by pressure. The small  $^Dv$  value is reasonable since the rate-limiting step is the release of THF from the DHFR•NADPH•THF complex at atmospheric pressure [12]. However, the pressure insensitivity of  $^Dv$  does not necessarily mean that the product-releasing process is the rate-limiting step at high pressure, since compression of the protein structure could affect the reaction pathways.

(Table 2)

### 3.3. Dissociation constants of ligands

Fig. 4 shows the folate concentration dependence of the fluorescence spectra of DHFR at 200 MPa. Similar changes in the spectra with the ligand

concentration were observed at other pressures for all ligands tested (data not shown). The intensity of each spectrum at the peak wavelength of the 0.1-MPa spectrum was plotted as a function of ligand concentration, with a typical result shown in the inset of Fig. 4. The values of  $K_d$  obtained by curve fitting with Eq. 6 are listed in Table 3.  $K_d$  increased with the pressure for all ligands, indicating that pressure facilitates the dissociation of ligands from the enzyme for volume reductions. The dissociation constant of NADP<sup>+</sup> from the DHFR•NADP<sup>+</sup>•THF ternary complex was not obtained since no significant change in fluorescence spectra was evident for the DHFR•NADP<sup>+</sup> and DHFR•THF binary complexes.

(Fig. 4) (Table 3)

Fig. 5 plots the Gibbs free energy change of ligand dissociation,  $\Delta G_d$ , against pressure, indicating the highly linear relationships for pressures above 50 MPa. The volume changes due to dissociation,  $\Delta V_d$ , were calculated from the slopes (Eq. 9), and the results are listed in the last column of Table 3. Dissociation of substrates (folate, DHF, and THF) from DHFR produced volume decreases from 6.5 ml mol<sup>-1</sup> (THF) to 13.4 ml mol<sup>-1</sup> (folate), with these decreases becoming smaller for dissociation from the ternary complex. On the other hand, dissociation of cofactors NADP<sup>+</sup> and NADPH from DHFR produced much larger volume decreases of 20.7 and 33.5 ml mol<sup>-1</sup>, respectively. A comparable volume decrease of 28 ml mol<sup>-1</sup> occurred on dissociation of NADPH from the ternary complex. These values reflect the volume change of not only protein and ligands but also whole system, including volume change of hydrated water. Since several hundreds or a thousand of hydrated water molecules hydrate a protein and ligand molecule, binding of a ligand to DHFR generate dehydration of many water molecules, which are contribute to the  $\Delta V_d$  values [24]. Evidently, the  $\Delta G_d$  values for many ligands at 0.1 MPa deviate from the linear fits above 50 MPa: downward for DHF (Fig. 5A) and NADP<sup>+</sup> (Fig. 5B), and upward for folate (Fig. 5C). These results suggest that the conformation of DHFR differs between pressures below and above around 50 MPa.

(Fig. 5)

## 4. Discussion

The present study has revealed that the enzymatic function of DHFR is depressed at high pressure. As shown in Scheme 1, there are several equilibrium and kinetics processes in the enzyme reaction of DHFR that could be influenced by pressure. Although this reaction pathway was determined from the enzyme kinetics at atmospheric pressure [12], considering the volume changes of these equilibrium and kinetics processes is useful for understanding the pressure depression mechanism of the enzyme function.

### 4.1. Effects of pressure on the equilibrium reaction

From the volume changes of ligand dissociation (Table 3), we estimated the volume levels of five major intermediates (DHFR•NADPH, DHFR•NADPH•DHF, DHFR•NADP<sup>+</sup>•THF, DHFR•THF, and DHFR•NADPH•THF) relative to the volume of apoenzyme (DHFR). The assumed volume level of each intermediate is shown along the reaction coordinate in Fig. 6. The volume levels of two ternary complexes, DHFR•NADPH•DHF and DHFR•NADP<sup>+</sup>•THF, were assumed as described below since measuring  $\Delta V_d$  was difficult for the dissociation of DHF from the transient state DHFR•NADPH•DHF and for the dissociation of THF from DHFR•NADP<sup>+</sup>•THF due to there being no significant fluorescence change. The volume level of DHFR•NADPH•DHF was estimated to be 40.8 ml mol<sup>-1</sup> from the sum of the volume increase (7.3 ml mol<sup>-1</sup>) of folate binding to DHFR•NADPH and the volume increase of DHFR•NADPH (33.5 ml mol<sup>-1</sup>), because the  $\Delta V_d$  values of folate and DHF (-13.4 and -12.7 ml mol<sup>-1</sup>, respectively) were similar in their binary complexes (Table 3). The volume level of DHFR•NADP<sup>+</sup>•THF was estimated to be 27.2 ml mol<sup>-1</sup> by adding the volume increases of THF and NADP<sup>+</sup> binding (6.5 and 20.7 ml mol<sup>-1</sup>, respectively) to that of the apoenzyme. The volume level of DHFR•NADPH•THF was considered to be the mean (35.6 ml mol<sup>-1</sup>) of the two volume increases (36.5 and 34.8 ml mol<sup>-1</sup>) that were estimated

respectively by adding the volume changes for the two processes of (DHFR+NADPH) and (DHFR•NADPH+THF) and of (DHFR+THF) and (DHFR•THF+NADPH). Although these volume levels involve considerable experimental errors and some assumptions, they are useful for surveying the effects of pressure on the equilibrium processes of the enzyme reaction.

(Fig. 6)

Fig. 6 shows that the volume of the intermediate alternately increases and decreases depending on the binding and releasing of substrates and cofactors, with DHFR•NADPH•DHF and DHFR•THF being the most voluminous and compact of the intermediates, respectively. This volume profile is similar to the compressibility profile, where the transient state is the most compressible [13]. There are two volume-increasing processes evident: binding of DHF to DHFR•NADPH and binding of NADPH to DHFR•THF. These ligand-binding processes are depressed by pressure, with the effect being larger for the latter process. On the other hand, there are three volume-decreasing processes that are enhanced by pressure: (i) the dissociation of NADP<sup>+</sup> from DHFR•NADP<sup>+</sup>•THF, (ii) the dissociation of THF from DHFR•NADPH•THF, and (iii) the hydride transfer from DHFR•NADPH•DHF to DHFR•NADP<sup>+</sup>•THF. The formation of the enzyme•ligand complex is generally considered to proceed through three states: (i) formation of new bonds between enzyme and ligand, (ii) changes in hydration of the interacting species, and (iii) conformational changes of the enzyme. These processes should produce volume changes mainly via changes in internal atomic packing (cavity) and the amount of hydration. Quantitatively evaluating these two contributions is difficult and outside the scope of the present study, but the volume increase on ligand binding or the volume decrease on ligand dissociation would be mainly attributable to changes in the hydration of enzyme and ligands because the volume change due to hydration is negative. In this respect, it is noteworthy that the hydride transfer produces a large volume decrease (of about 13 ml mol<sup>-1</sup>) despite only a single hydrogen atom being transferred from NADPH to DHF. Considering the  $\Delta V_d$  data in Table 3, about half (6 ml mol<sup>-1</sup>) of this volume decrease may be attributed to the transformation of DHF to THF, with the

other half (7 ml mol<sup>-1</sup>) being attributed to the transformation of NADPH to NADP<sup>+</sup>. Thus, these two processes would be comparably affected by pressure.

#### 4.2. Effects of pressure on the kinetics process

The enzyme activity is determined not only by the equilibrium reactions (affinity of substrates and cofactors) but also – and more dominantly – by the kinetics processes between the intermediates. Therefore, the activation volume for each process is important for the effects of pressure on the enzyme function. There are at least five kinetics processes in the enzyme reaction (Scheme 1), with the dissociation of THF from DHFR•NADPH•THF being the rate-limiting step at atmospheric pressure [12]. In the present study we determined only the activation volume for the overall enzyme reaction ( $\Delta V^* = 7.8$  ml mol<sup>-1</sup>), which corresponds to that for the rate-limiting process in the reaction pathway. However, the rate-limiting step at high pressure may differ from that at atmospheric pressure since the plots of  $\Delta G_a$  vs. pressure of many ligands were kinked at 0–50 MPa, and hence it is pertinent to consider the rate-limiting step from the volume relationship.

*Substrate- and cofactor-binding processes* – As shown in Fig. 6, there are two volume-increasing processes. The volume increase for DHF binding to DHFR•NADPH (7.3 ml mol<sup>-1</sup>) is comparable with  $\Delta V^*$ , and NADPH binding to DHFR•THF produces a large volume increase of more than 7.8 ml mol<sup>-1</sup>; therefore, neither of these two processes would be the rate-limiting step. If the substrate- or cofactor-binding process is the rate-limiting step, the reaction rate should depend on the concentration of substrate or cofactor. However, the  $\Delta V^*$  values were almost same at different substrate and cofactor concentrations:  $8.1 \pm 0.8$  ml mol<sup>-1</sup> for 50  $\mu$ M [15] and  $7.8 \pm 0.6$  ml mol<sup>-1</sup> for 250  $\mu$ M (this study). Further, the  $K_m$  values were only slightly higher at 200 MPa than at atmospheric pressure (Table 1). These results indicate that DHF- and NADPH-binding steps are not the rate-limiting step at high pressure.

*Hydride-transfer process* – The hydride transfer from DHFR•NADPH•DHF to DHFR•NADP<sup>+</sup>•THF, which is both a chemical and

catalytic reaction, is known to be the fastest process in the reaction pathway of this enzyme (Scheme 1). As shown in Fig. 6, this process produces a volume reduction, but a positive activation volume may be possible for its kinetics process. However, Northrop and coworkers recently showed that the reduction of NAD<sup>+</sup> by alcohol and formate dehydrogenases was accelerated at high pressure, with activation volumes of  $-38 \pm 1$  and  $-9.3 \pm 1.1$  ml mol<sup>-1</sup>, respectively [25, 26]. This suggests that the  $\Delta V^*$  value should be negative for the hydride-transfer process, given that DHFR•NADPH•DHF has a higher volume than DHFR•NADP<sup>+</sup>•THF. The small and pressure-insensitive  $\Delta V$  values (Table 2) also indicate that the hydride transfer is not the rate-limiting step at high pressure.

*Substrate- and cofactor-releasing processes* – The releases of NADP<sup>+</sup> from DHFR•NADP<sup>+</sup>•THF and of THF from DHFR•NADPH•THF accompany the volume decrease, and hence a positive activation volume may be possible for their kinetics processes. However, we were unable to determine which of them is the rate-limiting process at high pressure because no kinetics experiment was performed for the releasing processes of these ligands.

#### 4.3. Effects of pressure on enzyme conformation

As shown in Fig. 5, the  $\Delta G_d$  values observed at 0.1 MPa deviate from the extrapolation of the data at 50–200 MPa for most of the ligand systems, suggesting that some conformational change of the enzyme occurs at pressures above 50 MPa. A high-pressure NMR study [3] revealed that a transformation from the ‘closed’ to the ‘open’ conformer is induced by pressure in the DHFR•folate binary complex with a volume decrease of 25 ml mol<sup>-1</sup>. This suggests that such a conformational change of the enzyme also occurs in the transient state DHFR•NADPH•DHF. If this is the case and the volume decrease is much smaller than 7.8 ml mol<sup>-1</sup>, this conformational change could be the rate-limiting step of the enzyme reaction. Cameron and Benkovic [27] reported that the conformational conversion in DHFR•NADPH•DHF is the rate-limiting step for the G121V mutant of DHFR, whose enzyme activity is 26-fold smaller than that of the wild type [4]. Although it is unknown whether this conformational conversion is identical to the transformation from the ‘open’ to the ‘closed’ conformer, it is

possible that the rate-limiting step is the conformational change of the enzyme at high pressure.

As discussed above, many processes are complicatedly affected by pressure in the enzyme reaction of DHFR. Despite the limited availability of kinetics data, the present study provides the first evidence of the volume levels of the intermediates and three candidates for the rate-limiting process: two are the releasing processes of THF and NADP<sup>+</sup>, and the third is the conformational transition of the enzyme. Detailed investigations of the kinetics at high pressure are required to determine the activation volume for each step in the reaction pathway of DHFR. The resulting data will help to elucidate the pressure adaptation mechanism of DHFRs from deep-sea bacteria.

### **Acknowledgements**

We thank the Academic Center for Computing and Media Studies of Kyoto University for the use of the SALS program. This work was financially supported by a Grant-in-Aid for Scientific Research from the Ministry of Education, Science, Sports, and Culture of Japan (No. 16657031).



## References

- [1] J.R. Schnell, H.J. Dyson, P.E. Wright, Structure, dynamics, and catalytic function of dihydrofolate reductase, *Annu. Rev. Biophys. Biomol. Struct.* 33 (2004) 119–140.
- [2] M.R. Sawaya, J. Kraut, Loop and subdomain movements in the mechanism of *Escherichia coli* dihydrofolate reductase: crystallographic evidence, *Biochemistry* 36 (1997) 586–603.
- [3] R. Kitahara, S. Sareth, H. Yamada, E. Ohmae, K. Gekko, K. Akasaka, High pressure NMR reveals active-site hinge motion of folate-bound *Escherichia coli* dihydrofolate reductase, *Biochemistry* 39 (2000) 12789–12795.
- [4] K. Gekko, Y. Kunori, H. Takeuchi, S. Ichihara, M. Kodama, Point mutations at glycine-121 of *Escherichia coli* dihydrofolate reductase: important roles of a flexible loop in the stability and function, *J. Biochem. (Tokyo)* 116 (1994) 34–41.
- [5] E. Ohmae, K. Iriyama, S. Ichihara, K. Gekko, Effects of point mutations at the flexible loop glycine-67 of *Escherichia coli* dihydrofolate reductase on its stability and function, *J. Biochem. (Tokyo)* 119 (1996) 703–710.
- [6] E. Ohmae, K. Ishimura, M. Iwakura, K. Gekko, Effects of point mutations at the flexible loop alanine-145 of *Escherichia coli* dihydrofolate reductase on its stability and function, *J. Biochem. (Tokyo)* 123 (1998) 839–846.
- [7] S. Kunugi, M. Kitayaki, Y. Yanagi, N. Tanaka, R. Lange, C. Balny, The effect of high pressure on thermolysin, *Eur. J. Biochem.* 248 (1997) 567–574.
- [8] S. Fujiwara, S. Kunugi, H. Oyama, K. Oda, Effects of pressure on the activity and spectroscopic properties of carboxyl proteinases. Apparent correlation of pepstatin-insensitivity and pressure response, *Eur. J. Biochem.* 268 (2001) 645–655.
- [9] D.B. Northrop, Effects of high pressure on enzymatic activity, *Biochem. Biophys. Acta* 1595 (2002) 71–79.
- [10] P. Masson, C. Balny, Linear and non-linear pressure dependence of enzyme catalytic parameters, *Biochem. Biophys. Acta* 1724 (2005) 440–450.

- [11] C. Balny, What lies in the future of high-pressure bioscience? *Biochem. Biophys. Acta* 1764 (2006) 632–639.
- [12] C.A. Fierke, K.A. Johnson, S.J. Benkovic, Construction and evaluation of the kinetic scheme associated with dihydrofolate reductase from *Escherichia coli*, *Biochemistry* 26 (1987) 4085–4092.
- [13] T. Kamiyama, K. Gekko, Effect of ligand binding on the flexibility of dihydrofolate reductase as revealed by compressibility, *Biochim. Biophys. Acta* 1478 (2000) 257–266.
- [14] D.D. Boehr, D. McElheny, H.J. Dyson, P.E. Wright, The dynamic energy landscape of dihydrofolate reductase catalysis, *Science* 313 (2006) 1638–1642.
- [15] E. Ohmae, K. Kubota, K. Nakasone, C. Kato, K. Gekko, Pressure-dependent activity of dihydrofolate reductase from a deep-sea bacterium *Shewanella violacea* strain DSS12, *Chem. Lett.* 33 (2004) 798–799.
- [16] M. Iwakura, B.E. Jones, J. Luo, C.R. Matthews, A strategy for testing the suitability of cysteine replacements in dihydrofolate reductase gene from *Escherichia coli*, *J. Biochem. (Tokyo)* 117 (1995) 480–488.
- [17] R.M.C. Dawson, D.C. Elliot, W.H. Elliot, K.M. Jones, In: *Data for Biochemical Research*, Oxford University Press, Oxford, 1969.
- [18] J.W. Williams, J.F. Morrison, R.G. Duggleby, Methotrexate, a high-affinity pseudosubstrate of dihydrofolate reductase, *Biochemistry* 18 (1979) 2567–2573.
- [19] S.R. Stone, J.F. Morrison, Kinetic mechanism of the reaction catalyzed by dihydrofolate reductase from *Escherichia coli*, *Biochemistry* 21 (1982) 3757–3765.
- [20] M.H. Penner, C. Frieden, Substrate-induced hysteresis in the activity of *Escherichia coli* dihydrofolate reductase, *J. Biol. Chem.* 260 (1985) 5366–5369.
- [21] G.L. Atkins, I.A. Nimmo, The reliability of Michaelis constants and maximum velocities estimated by using the integrated Michaelis–Menten equation, *Biochem. J.* 135 (1973) 779–784.
- [22] C.T. Goudar, S.K. Harris, M.J. McInerney, J.M. Suflita, Progress curve analysis for enzyme and microbial kinetic reactions using explicit solutions based on the Lambert  $W$  function, *J. Microbiol. Methods* 59

(2004) 317–326.

- [23] T. Nakagawa, Y. Oyanagi, In: K. Matsushita (ed.), *Recent Developments in Statistical Inference and Data Analysis*, North Holland Publishing, Amsterdam, 1980, pp. 221–225.
- [24] E. Ohmae, C. Murakami, K. Gekko, C. Kato, Pressure effects on enzyme functions, *J. Biol. Macromol.* 7 (2007) 23-29.
- [25] D.B. Northrop, Y.K. Cho, Effects of pressure on deuterium isotope effects of yeast alcohol dehydrogenase: evidence for mechanical models of catalysis, *Biochemistry* 39 (2000) 2406–2412.
- [26] D.J. Quirk, D.B. Northrop, Effect of pressure on deuterium isotope effects of formate dehydrogenase, *Biochemistry* 40 (2001) 847–851.
- [27] C.E. Cameron, S.J. Benkovic, Evidence for a functional role of the dynamics of glycine-121 of *Escherichia coli* dihydrofolate reductase obtained from kinetic analysis of a site-directed mutant, *Biochemistry* 36 (1997) 15792–15800.
- [28] C. Bystroff, S.J. Oatley, J. Kraut, Crystal structures of *Escherichia coli* dihydrofolate reductase: the NADP<sup>+</sup> holoenzyme and the folate-NADP<sup>+</sup> ternary complex. Substrate binding and a model for the transition state, *Biochemistry* 29 (1990) 3263–3277.
- [29] W.L.T. DeLano, *The PyMOL Molecular Graphics System*, DeLano Scientific, San Carlos, CA, USA, 2002.

Table 1

Apparent kinetics parameters for the enzyme reaction of DHFR at 0.1 and 200 MPa. <sup>a</sup>

Parameter	NADPH		DHF	
	0.1 MPa	200 MPa	0.1 MPa	200 MPa
$[S]_0$ ( $\mu\text{M}$ )	$26.1 \pm 0.1$	$16.3 \pm 0.1$	$28.3 \pm 0.1$	$15.5 \pm 0.1$
$K_m$ ( $\mu\text{M}$ )	$17.8 \pm 0.9$	$19.5 \pm 1.6$	$3.1 \pm 0.1$	$4.6 \pm 0.3$
$v_{\max}$ ( $\text{nM s}^{-1}$ )	$164 \pm 4$	$164 \pm 9$	$95 \pm 1$	$93 \pm 2$
$A$	$0.379 \pm 0.001$	$0.411 \pm 0.001$	$0.364 \pm 0.000$	$0.382 \pm 0.000$

<sup>a</sup> The parameters were conventionally obtained by fitting the time course of absorbance with Eqs. 3 and 4. The solvent was 20 mM Tris-hydrochloride (pH 7.0) containing 0.1 mM EDTA and 0.1 mM dithiothreitol.

Table 2

Effect of deuterium isotope ( $D_V$ ) on the enzyme reaction of DHFR at various pressures. <sup>a</sup>

Pressure (MPa)	$D_V$
0.1	$1.2 \pm 0.1$
50	$1.2 \pm 0.1$
100	$1.2 \pm 0.0$
150	$1.1 \pm 0.0$
200	$1.1 \pm 0.0$
250	$1.1 \pm 0.0$

<sup>a</sup>  $D_V$  was calculated with Eq. 5. The buffer used was 20 mM Tris-hydrochloride (pH 7.0) containing 0.1 mM EDTA, 0.1 mM dithiothreitol, 250  $\mu$ M DHF, and 250  $\mu$ M NADPH or NADPD.

Table 3

Equilibrium dissociation constants ( $K_d$ ) of ligand from DHFR and DHFR•ligand complexes at various pressures and volume changes of dissociation ( $\Delta V_d$ ) at 25 °C and pH 7.0.

Protein	Ligand	$K_d$ ( $\mu\text{M}$ )					$\Delta V_d$ (ml mol <sup>-1</sup> )
		0.1 MPa	50 MPa	100 MPa	150 MPa	200 MPa	
DHFR	Folate	1.5 ± 0.2	2.1 ± 0.1	2.7 ± 0.1	3.7 ± 0.2	4.6 ± 0.3	-13.4 ± 0.6
	DHF	1.4 ± 0.2	1.3 ± 0.2	1.6 ± 0.2	2.1 ± 0.2	2.8 ± 0.3	-12.7 ± 0.3
	THF	3.8 ± 1.0	4.0 ± 0.2	4.5 ± 0.3	5.0 ± 0.3	6.6 ± 0.9	-6.5 ± 1.1
	NADP <sup>+</sup>	15.0 ± 2.3	15.3 ± 1.9	22.9 ± 2.8	34.3 ± 3.0	54.7 ± 5.1	-20.7 ± 0.5
	NADPH	0.1 ± 0.1	0.2 ± 0.1	0.3 ± 0.1	0.6 ± 0.2	1.3 ± 0.3	-33.5 ± 2.0
DHFR•NADPH	Folate	3.6 ± 0.6	5.9 ± 0.2	7.1 ± 0.2	8.1 ± 0.3	9.3 ± 0.3	-7.3 ± 0.4
	THF	9.7 ± 0.5	10.4 ± 0.3	11.5 ± 0.3	11.7 ± 0.3	12.4 ± 0.4	-3.0 ± 0.4
DHFR•folate <sup>a</sup>	NADPH	0.3 ± 0.4	0.5 ± 0.3	0.8 ± 0.3	1.3 ± 0.3	2.7 ± 0.3	-28.2 ± 1.9
DHFR•THF <sup>a</sup>	NADPH	0.4 ± 0.1	0.4 ± 0.2	0.8 ± 0.1	1.4 ± 0.2	2.5 ± 0.1	-28.3 ± 0.6

<sup>a</sup> Dissociation constants of ligands from these DHFR•ligand complexes were calculated by linked function analysis according to the thermodynamics of cyclic equilibria (see Materials and Methods). The solvent was 20 mM Tris-hydrochloride (pH 7.0) containing 0.1 mM EDTA and 0.1 mM dithiothreitol.

## Legends for Figures and Scheme

Fig. 1. Drawing of the backbone ribbon of the DHFR•NADPH•folate complex (PDB code: 7DFR). Taken from Bystroff *et al.* [28]. NADPH and folate are drawn as a stick model. This figure was drawn using PyMOL [29] (<http://pymol.sourceforge.net/>).

Fig. 2. Time courses of absorbance at 370 nm due to the enzyme reaction of DHFR at 25°C and pH 7.0 at various pressures. The solvent used was 20 mM Tris-hydrochloride (pH 7.0) containing 0.1 mM EDTA, 0.1 mM dithiothreitol, 250  $\mu$ M NADPH, and 250  $\mu$ M DHF. The dead time of the measurement was 1 min. Pressures: 0.1 MPa (a), 50 MPa (b), 100 MPa (c), 150 MPa (d), 200 MPa (e), and 250 MPa (f). Arrow indicates decompression from 250 to 0.1 MPa. Inset: Pressure dependence of the  $\Delta G^*$  values of the enzyme reaction of DHFR calculated with Eq. 2. Solid line indicates a linear fit.

Fig. 3. Time courses of absorbance at 340 nm due to the enzyme reaction of DHFR at 25°C and pH 7.0 at 0.1 and 200 MPa. The solvent used was 20 mM Tris-hydrochloride (pH7.0) containing 0.1 mM EDTA and 0.1 mM dithiothreitol. Data points are every 10 s. Solid lines indicate curves fitted with Eqs. 3 and 4. (A): Reactions with 30  $\mu$ M NADPH and 80  $\mu$ M DHF at 0.1 MPa ( ) and 200 MPa ( ). (B): Reactions with 30  $\mu$ M DHF and 80  $\mu$ M NADPH at 0.1 MPa ( ) and 200 MPa ( ).

Fig. 4: Folate concentration dependence of the fluorescence spectra of DHFR at 200 MPa. The solvent used was 20 mM Tris-hydrochloride (pH 7.0) containing 0.1 mM EDTA and 0.1 mM dithiothreitol. The folate concentration was 0, 1, 3, 5, 10, 15, 20, 30, 50, and 100  $\mu$ M (from top to bottom). Inset: Peak intensities against the folate concentrations at 0.1 ( ), 50 ( ), 100 ( ), 150 ( ), and 200 (x) MPa. Solid lines indicate nonlinear least-squares fits by Eq. 6.

Fig. 5. Pressure dependence of Gibbs free energy changes for the dissociation of ligands from DHFR or DHFR•ligand complexes at 25°C and pH 7.0. (A): Dissociations of DHF ( ), folate ( ), and THF ( ) from DHFR. (B):

Dissociations of NADPH ( ) and NADP<sup>+</sup> ( ) from DHFR. (C): Dissociations of folate ( ) and THF ( ) from DHFR•NADPH complex. (D): Dissociations of NADPH from DHFR•folate ( ) and DHFR•THF ( ) complexes. Solid lines indicate linear fits for the data points above 50 MPa except for folate in panel A and for THF in panel C, for which 0.1-MPa data were included in the fitting.

Fig. 6. Assumed volume levels of the kinetics intermediates along the reaction pathway of DHFR. The volume level of each intermediate was calculated from the  $\Delta V_a$  values listed in Table 3. The volume change of DHF binding to DHFR•NADPH binary complex was assumed to be same as that of folate binding to the complex. The volume level of DHFR•NADPH was depicted as the directly measured volume increase ( $33.5 \pm 2.0$  ml mol<sup>-1</sup>) since it was considered (within the experimental errors) to be identical to the value estimated by assuming the additivity of volume changes:  $31.8 \pm 1.3$  ml mol<sup>-1</sup> ( $= 6.5 + 28.3 - 3.0$ ). ‘E’ represents apo-DHFR.

Scheme 1. Steady-state enzyme kinetics of DHFR at atmospheric pressure. Rate constants were taken from Fierke *et al.* [12].



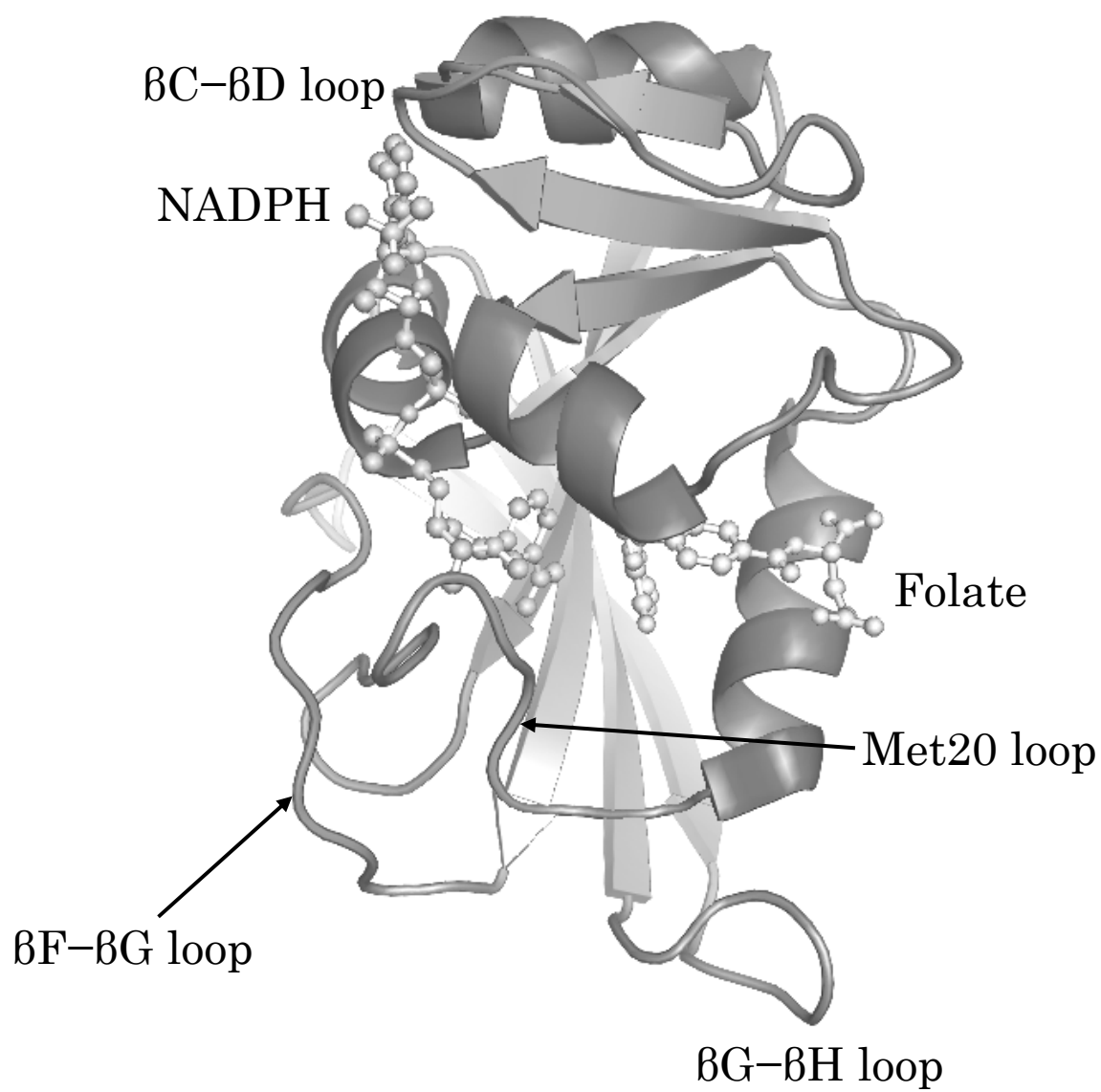


Figure 1: E. Ohmae *et al.*

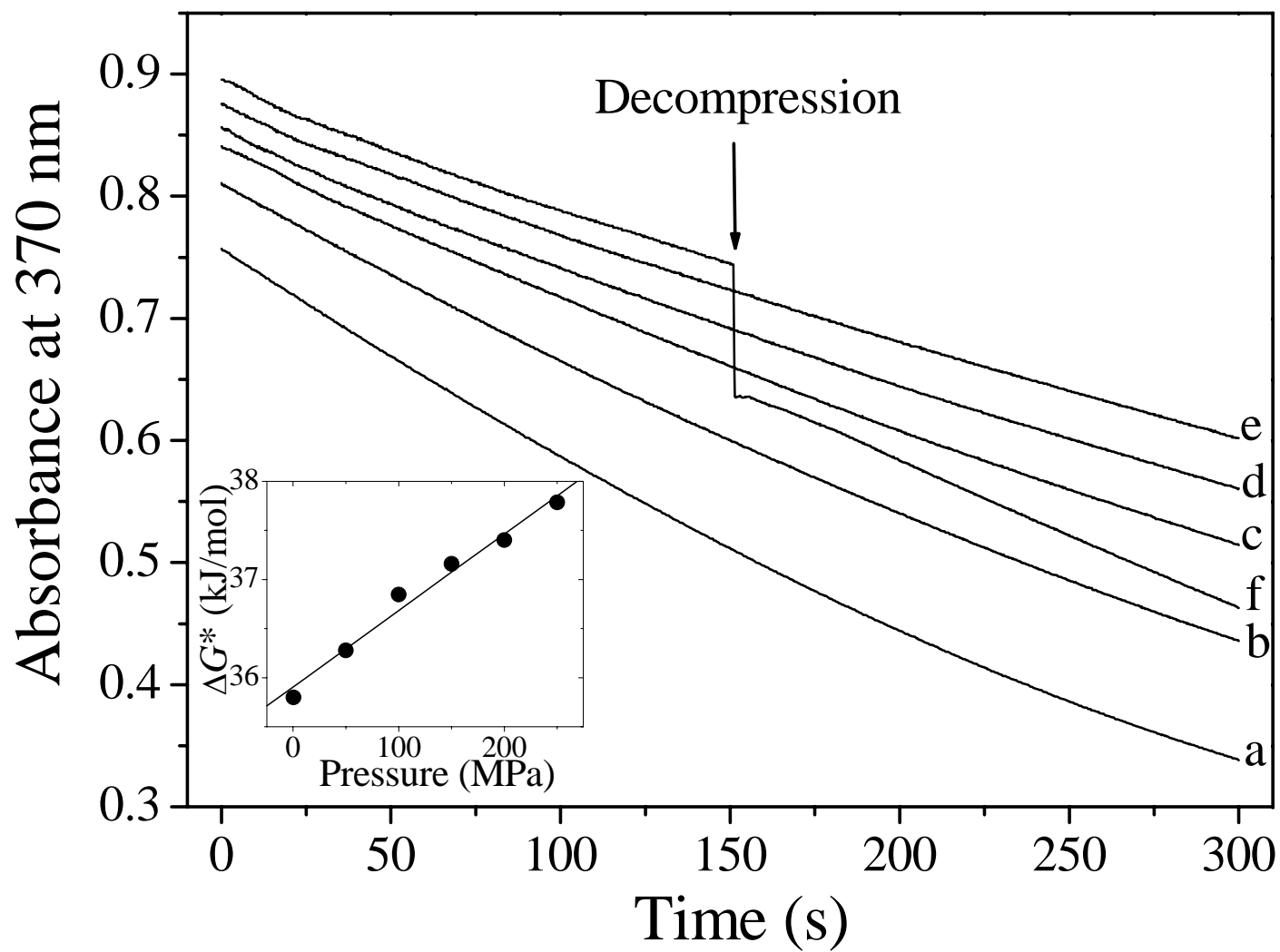


Figure 2: E. Ohmae *et al.*

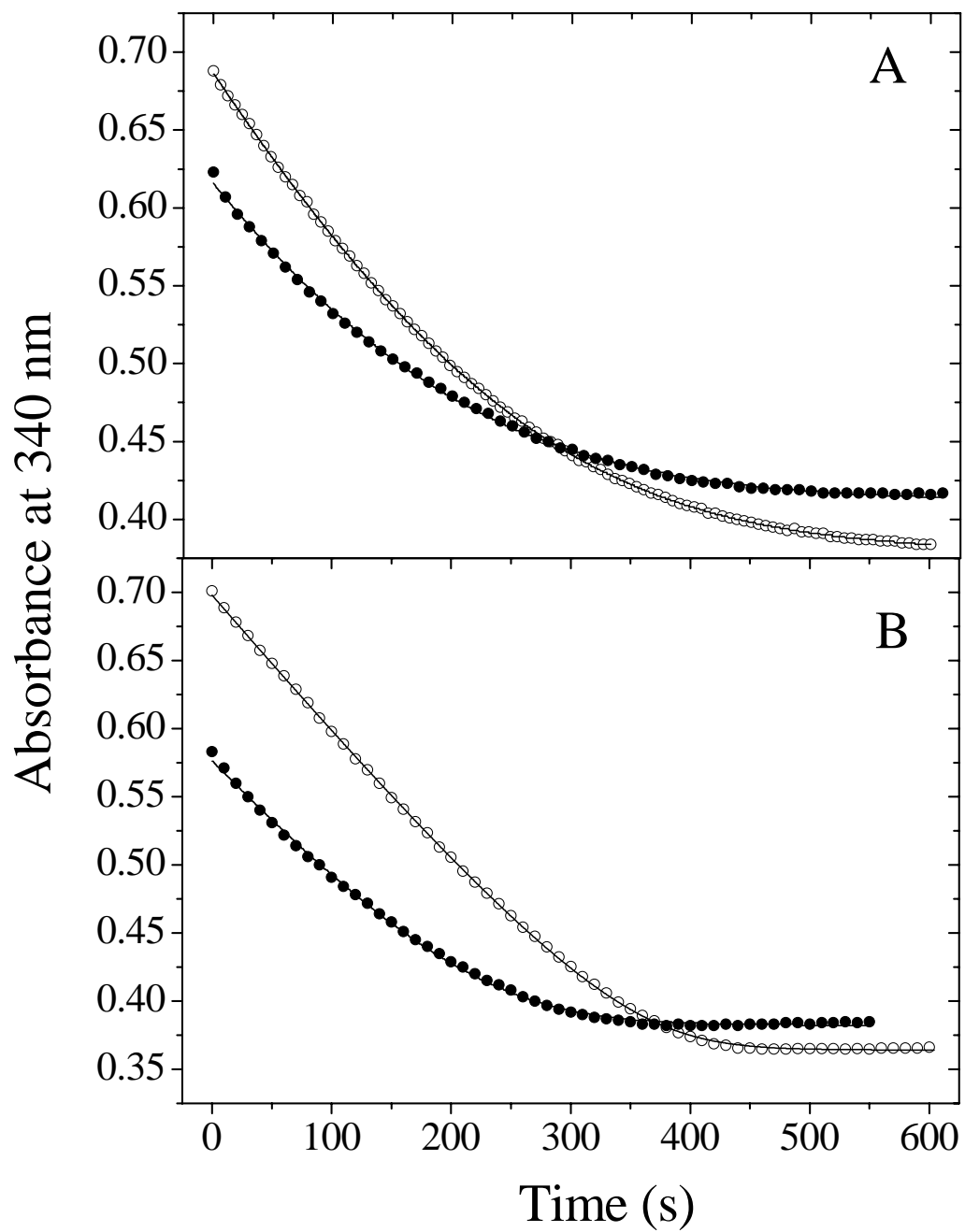


Figure 3: E. Ohmae *et al.*

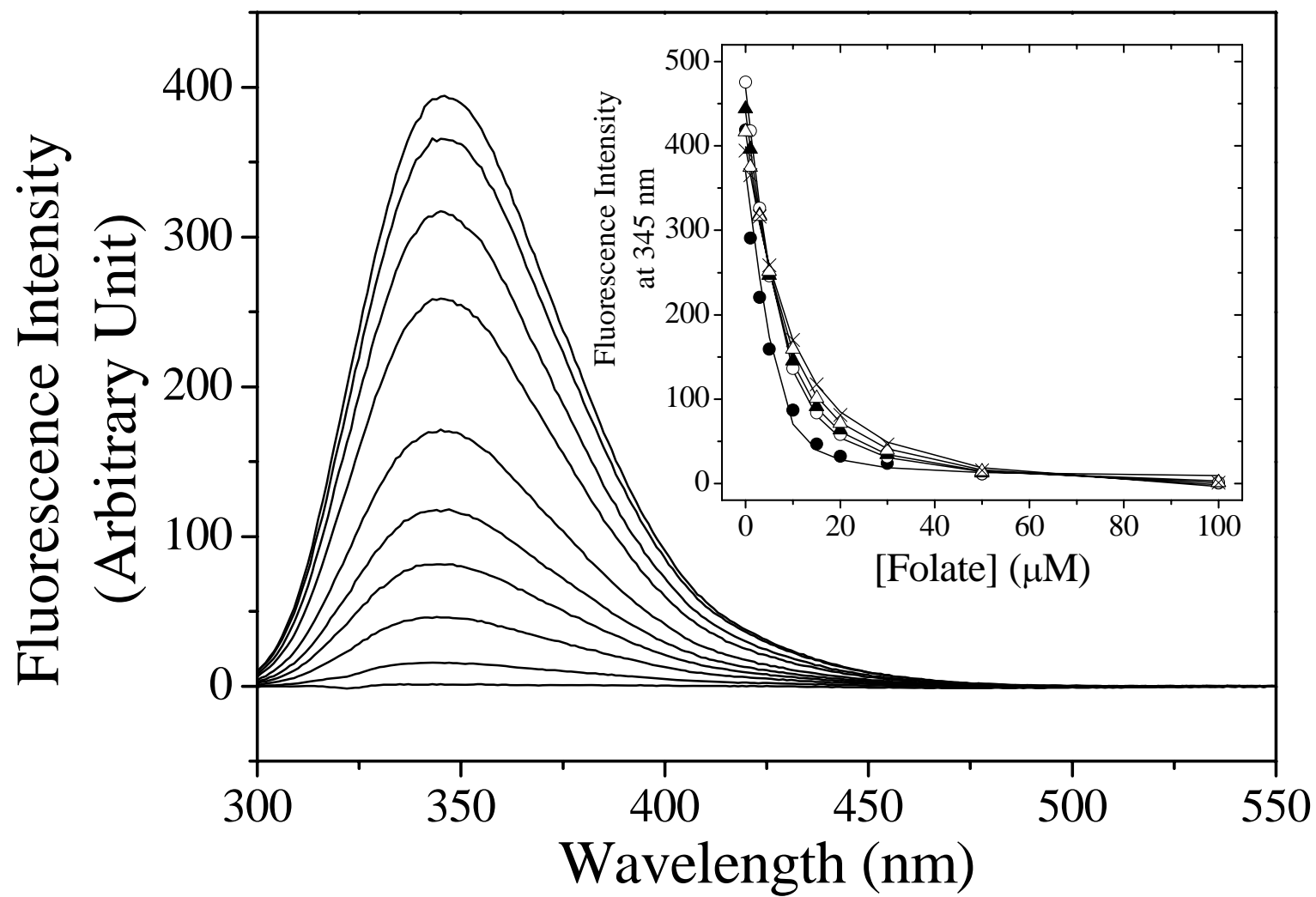


Figure 4: E. Ohmae *et al.*

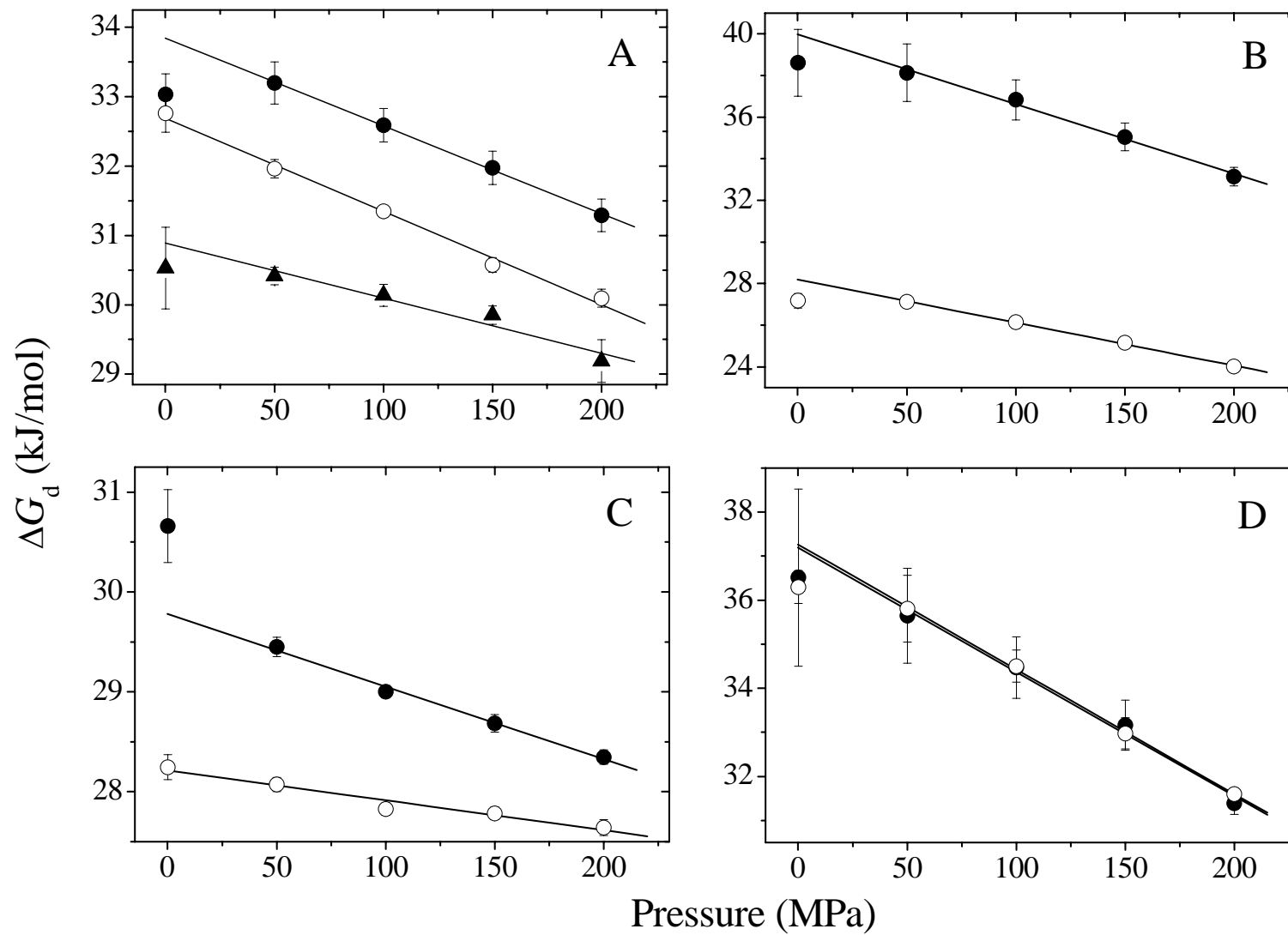


Figure 5: E. Ohmae *et al.*

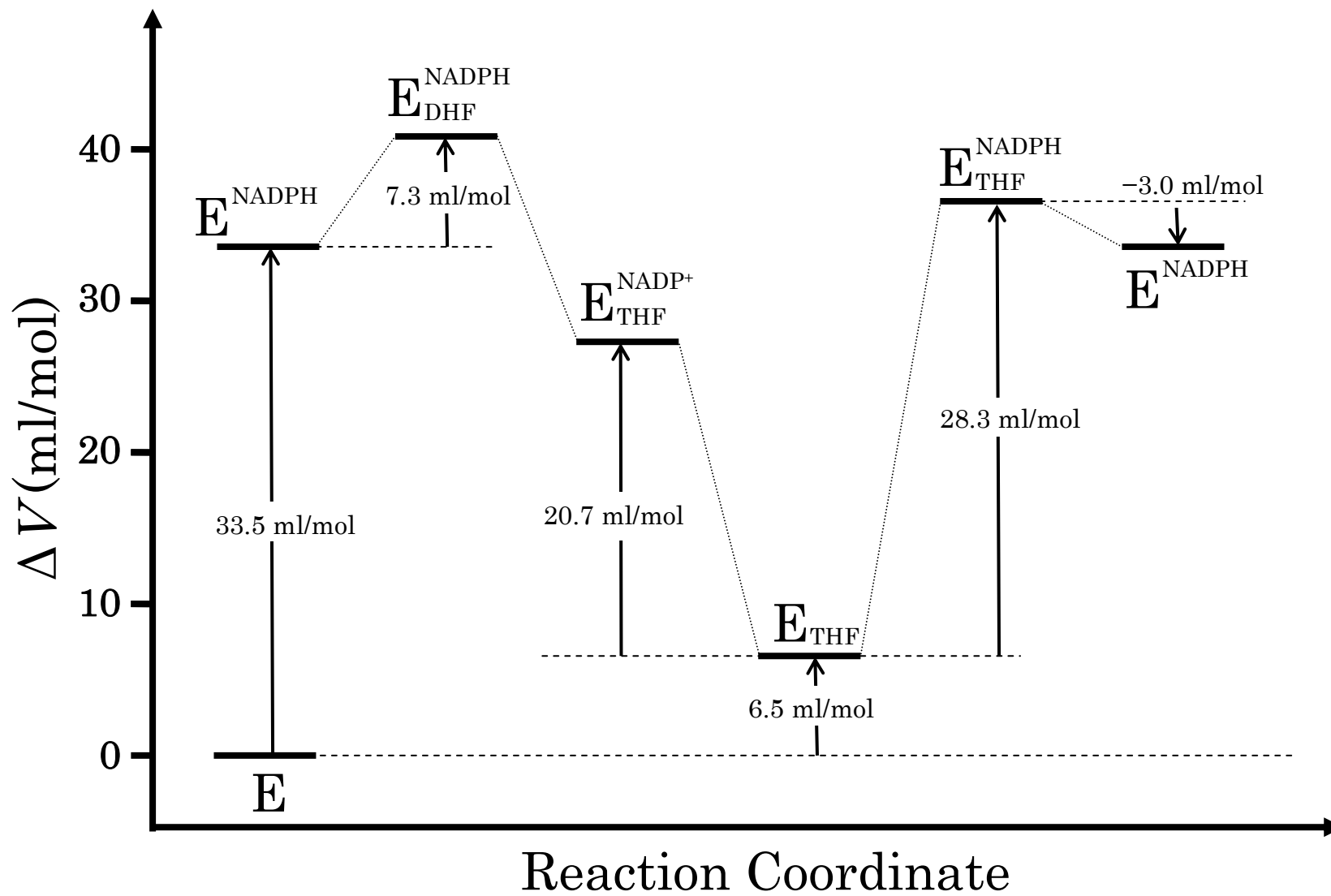
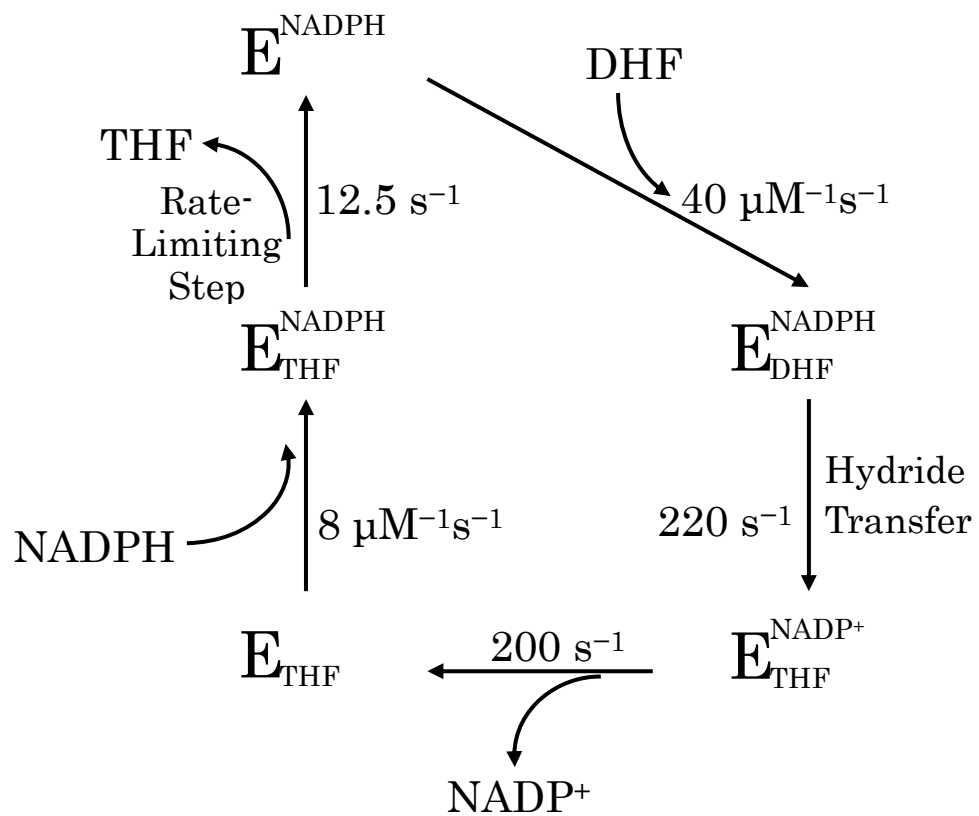


Figure 6: E. Ohmae *et al.*



Scheme 1: E. Ohmae *et al.*